

Measurement of the transport mean free path of diffusing photons

N. Garcia, A. Z. Genack, and A. A. Lisyansky

Department of Physics, Queens College of the City University of New York, Flushing, New York 11367

(Received 22 June 1992)

We measure microwave intensity *inside* and transmission through random samples of polystyrene spheres with different output reflectors. We show that with appropriate boundary conditions diffusion theory gives an excellent description of transport from the interior to the output surface of a sample. From these measurements we determine the transport mean free path and the surface reflectivities without additional assumptions regarding the interface or the scattering form factor. From a comparison with a measurement of the diffusion coefficient we determine the transport velocity and find that it is smaller than the velocity in the high-index material.

The particle diffusion model is widely used to describe the propagation of waves in multiply-scattering random media.¹⁻⁴ It has been applied to calculate the functional form of key aspects of electromagnetic propagation, such as surface intensity profiles³ which determine the shape of the coherent backscattering cone⁵⁻⁷ and angular correlation functions,^{8,9} the thickness dependence¹⁰ and temporal distribution of reflection¹¹ and transmission,¹² and spatial,¹³⁻¹⁷ spectral,^{10,13-18} and temporal^{19,20} correlation functions. Though qualitative agreement is obtained between experiment and theory, fundamental questions remain regarding the validity of the diffusion model as a quantitative description of wave transport. After all, diffusion is a local description, whereas the minimum scale on which transport can be described in terms of the average parameters which appear in the diffusion equation is the transport mean free path l , which is the length scale on which the direction of propagation is randomized. Moreover, l has not previously been unambiguously determined experimentally in the weak-scattering limit. In general the evaluation of l has involved a host of assumptions which are not inherent in diffusion theory. Determinations of l based upon static measurements depend upon interfacial properties such as the coefficient of the internal reflectivity²¹⁻²⁵ of the wave at the surface R , and the nature of the randomization of the propagation direction as the wave penetrates the sample,⁴ which depends upon the scattering form factor and the nature of the interface. The determination of l from measurements of the diffusion coefficient D in the time or frequency domains is also not feasible in general because D depends upon the effective transport velocity on a scale of the mean free path, $v = 3D/l$.²⁶ This velocity can be appreciably different from the phase velocity v_p whenever the scatterers are not much smaller than the wavelength, since the dwell time of photons within the scatterers can be enhanced by microstructure resonances.

In this paper, we report the measurement of the microwave intensity distribution *inside* and transmission through an ensemble of configurations of polystyrene spheres. These measurements are compared to predictions of the photon diffusion theory for samples with par-

tially reflecting boundaries. We find that the measurements are in agreement with the diffusion model with appropriate boundary conditions not only in the interior of the sample but also at the output surface of the sample. These results allow us to determine l , R , and v without making any additional assumptions regarding the nature of scattering.

The sample is a loose-packed collection of $\frac{1}{2}$ -in. polystyrene spheres at a volume filling fraction of 0.56. The spheres contain irregular air bubbles near their center which are approximately 4.5% of the sphere volume. The sample is 150 cm long and is contained between $\frac{1}{16}$ -in. plastic disks in two continuously rotated copper tubes separated by a thin stationary section, all with diameters of 7.3 cm. The tubes are rotated in order to tumble the sample to facilitate configuration averaging. A schematic of the experimental setup used to measure the intensity inside the sample is shown in Fig. 1.

The microwave radiation at 18.5 GHz emanates from a horn placed in the tube and facing the sample. A reflector is placed behind the horn to enhance the signal and to reduce the influence of small variations in the tube diameter upon the intensity in the sample. The intensity is detected using Schottky diode detectors. Intensity values reported are the average of measurements accumu-

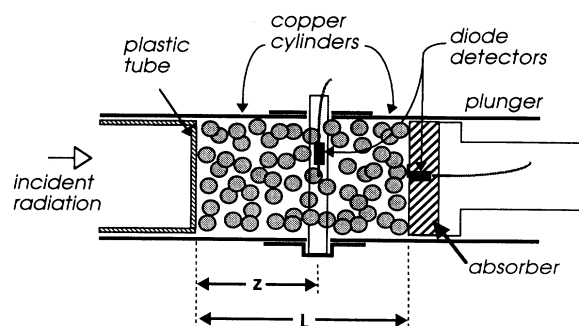


FIG. 1. Schematic of experimental setup used to measure the intensity profile inside the sample.

lated in $\frac{1}{2}$ h as the tubes rotate. Since the intensity correlation time in the tumbling sample is approximately 5 ms, this corresponds to the average of approximately 3×10^5 independent intensity measurements at each position.

Measurements of intensity inside the sample are made by placing a diode detector in a thin-walled plastic tube in the stationary section between the rotating copper tubes. The spacing of the detector from the output side of the sample is adjusted by moving the medium down the tubes while maintaining its overall length. This is done by translating the plastic tube at the input and the plunger at the output of the sample. Intensity measurements are made in the sample with only a plastic endpiece (output reflectivity R_1) and with additional reflecting copper plates placed in contact with the plastic disk at the output of the sample (reflectivities R_2 and R_3). These plates contain regularly spaced holes of $\frac{1}{2}$ -in. (R_2) and $\frac{1}{4}$ -in. (R_3) diameter, which cover approximately 55% and 42% of the plate area, respectively. The intensity measurements inside the sample for the three reflectivities at the output are shown in Fig. 2. The curves in the figure are a fit to the data using diffusion theory, which will be described shortly.

Relative measurements of transmission through the sample are also made for different boundary reflectors. The transmission depends upon the photon distribution and reflectivity at the output surface. The measurement is made by placing the output face of the sample at the input of a large box, which is mostly covered with roughened aluminum foil and serves as an "integrating box." This is shown schematically in Fig. 3. The un-

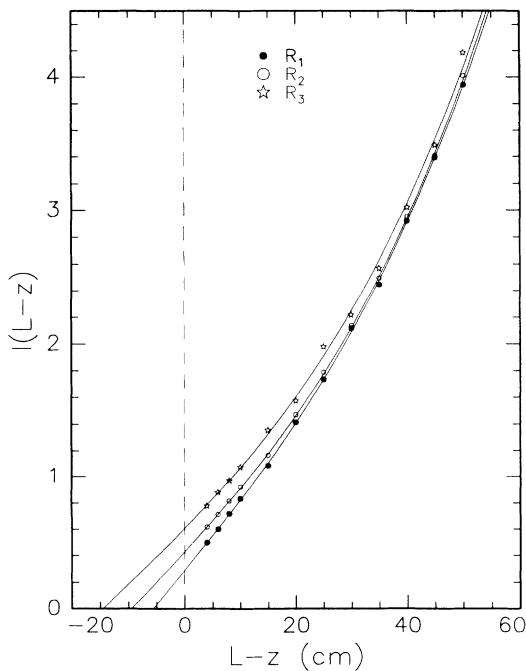


FIG. 2. Intensity profile inside a sample of randomly positioned $\frac{1}{2}$ -in. polystyrene spheres for three different reflectivities at the output of the sample. The solid lines are fits of Eqs. (3) and (8) to the data.

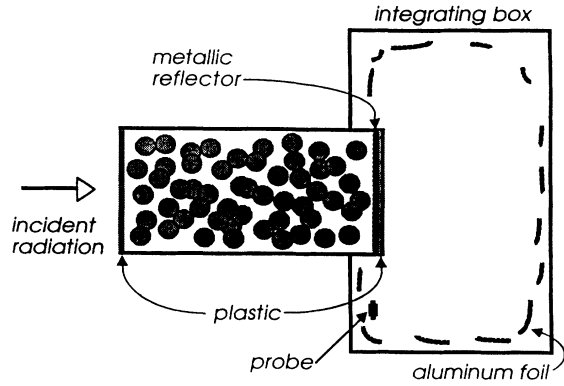


FIG. 3. Schematic of the experimental setup used to measure the relative transmission through the sample.

covered area is much larger than the cross-sectional area of the sample so that only a small fraction of the transmitted wave is reflected back into the sample. The amount of aluminum is reduced sufficiently that the presence of the "integrating" sphere does not influence the intensity inside the sample. Schottky diode detectors are placed near the input of the box, but in the shadow of the tube so that direct rays from the sample do not strike the detector. Measurements of transmission, \tilde{T} , in arbitrary units are given in Table I. A comparison of the intensity in Fig. 2 and the relative transmission in Table I will allow us to test diffusion theory and to find intrinsic propagation parameters in this sample.

Since the walls of the tube in our experiment are made of copper, which is a good reflector, the photon intensity distribution inside the tube is the same as in a slab of infinite transverse dimensions, provided that the sources of photons in both systems have the same intensity per

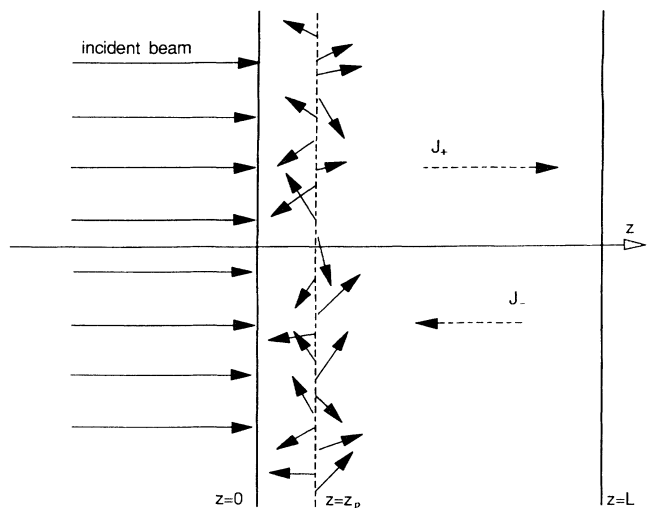


FIG. 4. Geometry used for the calculation of the intensity profile inside the slab of random media. A plane wave incident on the slab is replaced by a source of diffusive radiation positioned at distance z_p from the input.

TABLE I. Values of $\bar{T}(L)$, $\bar{I}(L^-)$, z_0 , and \bar{D} for three reflection coefficients.

	\bar{T}	z_0 (cm)	$\bar{I}(L^-)$	\bar{D}
R_1	0.400	5.93	0.290	8.17
R_2	0.378	9.3	0.430	8.17
R_3	0.366	13.9	0.606	8.40

unit area. We consider propagation through a slab of a random medium of infinite extent in the x, y directions situated between $0 < z < L$. We assume that we are in the weakly scattering regime in which $kl \gg 1$, where k is the magnitude of the photon wave vector, so that wave interference does not influence average transport. We calculate the intensity inside the slab $I(z)$ using the diffusion equation

$$\nabla^2 I(\mathbf{r}) - \alpha^2 I(\mathbf{r}) = -\frac{1}{D} Q(\mathbf{r}), \quad (1)$$

where α is the inverse absorption length and $Q(\mathbf{r})$ is the source function. We assume that the coherent radiation

incident on the slab becomes randomized within a distance z_p , which is shown in Fig. 4. We replace the incoming coherent flux by a source of diffusive radiation at the plane $z = z_p$ with a strength equal to the incident flux. The source function can be written as $Q(\mathbf{r}) = Q(x, y)\delta(z - z_p)$.

The diffusion equation can be solved once the boundary conditions are specified. Since we assumed that there is no incoming flux through the boundaries, the only flux going from the boundary toward the inside of the slab is the reflected part of the outgoing flux,^{23,24} i.e.,

$$\begin{aligned} J_+(z=0^+) &= -R_l J_-(z=0^+), \\ J_-(z=L^-) &= -R_r J_+(z=L^-), \end{aligned} \quad (2)$$

where R_l and R_r are reflection coefficients of the left (input) and right (output) boundaries, correspondingly. For the case of plane-wave incident radiation, the source function $Q(x, y)$ is a constant, $Q(x, y) = q$, and the solution of Eq. (1) with the boundary conditions (2) can be written in the form

$$\begin{aligned} I(z) &= \frac{q}{\alpha D} [(1 + \alpha^2 z_{0l} z_{0r}) \sinh(\alpha L) + \alpha(z_{0l} + z_{0r}) \cosh(\alpha L)]^{-1} \\ &\times \begin{cases} [\sinh(\alpha z) + \alpha z_{0l} \cosh(\alpha z)] \{ \sinh[\alpha(L - z_p)] + \alpha z_{0r} \cosh[\alpha(L - z_p)] \}, & z < z_p \\ [\sinh(\alpha z_p) + \alpha z_{0l} \cosh(\alpha z_p)] \{ \sinh[\alpha(L - z)] + \alpha z_{0r} \cosh[\alpha(L - z)] \}, & z > z_p \end{cases} \end{aligned} \quad (3)$$

where

$$z_{0l,0r} = \frac{2}{3} l \frac{1 + R_{l,r}}{1 - R_{l,r}}. \quad (4)$$

Usually boundary conditions for photon diffusion are written not for fluxes but for intensities. In this case it is incorrect to take zero intensity at the boundaries for diffuse photons inside the medium.^{1,2} To resolve this problem, an extrapolation length z_b beyond the boundary in which the intensity drops to zero is generally introduced. No such assumption is introduced *a priori* in obtaining Eq. (3). We can check, however, whether an extrapolation length exists for the solution of Eq. (3) by solving the following equations:

$$I(z = -z_{bl})|_{z < 0} = 0, \quad I(z = L + z_{br})|_{z > L} = 0, \quad (5)$$

where the subscripts l and r correspond to the left and right boundaries of the sample. We find that when $R_{l,r} < R_c$, where

$$R_c = (1 - 2\alpha l / 3) / (1 + 2\alpha l / 3), \quad (6)$$

Eqs. (5) have the solutions

$$z_{bl,br} = \frac{1}{2\alpha} \ln \left(\frac{1 + \alpha z_{0l,0r}}{1 - \alpha z_{0l,0r}} \right). \quad (7)$$

If, however, either R_l or R_r is greater than R_c , then the intensity extrapolated beyond the corresponding boundary never becomes zero, so that an extrapolation length does not exist.

For $R_l, R_r < R_c$, Eq. (3) for the intensity distribution can be simplified using Eq. (7) to give

$$I(z) = I(z_p) \begin{cases} \sinh[\alpha(z + z_{bl})] / \sinh[\alpha(z_p + z_{bl})], & z < z_p \\ \sinh[\alpha(L + z_{br} - z)] / \sinh[\alpha(L + z_{br} - z_p)], & z > z_p \end{cases} \quad (8)$$

with

$$I(z_p) = \frac{q}{\alpha D} \frac{\sinh[\alpha(z_p + z_{bl})] \sinh[\alpha(L + z_{br} - z_p)]}{\sinh[\alpha(L + z_{bl} + z_{br})]} \quad (9)$$

The total normalized transmission through the slab can be expressed as

$$\begin{aligned} T(L) &= \frac{J_{\text{transmitted}}(L)}{J_{\text{incident}}} \\ &= \frac{1 - R_r}{q} J_+(L^-) \\ &= \frac{1}{\alpha r_{br}} \frac{\sinh[\alpha(z_p + z_{bl})] \sinh(\alpha z_{br})}{\sinh[\alpha(L + z_{bl} + z_{br})]} \end{aligned} \quad (10)$$

In our experiments we change the reflection coefficient of the right boundary and report measurements for $z > z_p$ only. Thus in the comparison of the theory to the experiment the terms in Eqs. (8) and (9) containing z_{bl} are constant, which can be combined as a single fitting parameter. The fit will yield the values of R_r , z_{0r} , and z_{br} for different boundary conditions. The subscript r will therefore be dropped in the discussion which follows. We also note that in the case of a planewave incident on a slab of a disordered medium in the absence of absorption and reflection diffusion theory gives $z_b = 2l/3$, whereas transport theory gives the Milne result $z_b = 0.7104l$.^{1,2} In the comparison of theory and experiment below we change the prefactor $2l/3$ in Eq. (4) to $0.7104l$.

We can fit Eqs. (3) and (8) independently to the experimental data in Fig. 2. We use z_0 and α as fitting parameters to Eq. (3) and z_b and α as fitting parameters to Eq. (8). The two fits almost exactly coincide and are shown by the lines in Fig. 2. The values of z_0 and α , and z_b and α obtained from the fits for different reflectors are given in Table II. The values of the absorption coefficient found from both fits coincide within experimental uncertainty. Using values of z_0 and α from the second and third columns of Table II, one can obtain values of z_b from Eq. (7). These values coincide with the experimental values of z_b given in the fourth column.

The mean free path can be obtained from z_0 using Eq. (4), but the reflection coefficient must be known. To determine the reflection coefficient we have measured the relative transmission for three different reflectors. The reflection coefficients can be obtained by comparing the values of z_0 and of the relative transmission for two different reflectors. We obtain a system of equations for the reflection coefficients from Eqs. (4) and (10),

TABLE II. Values of z_0 and α and z_b and α obtained from fitting Eqs. (3) and (8), respectively.

	z_0 (cm)	α (cm ⁻¹)	z_b (cm)	α (cm ⁻¹)
R_1	5.93±0.21	0.0259±0.0007	5.98±0.20	0.0259±0.0007
R_2	9.30±0.20	0.0272±0.0004	9.50±0.24	0.0272±0.0004
R_3	13.9±1.1	0.0263±0.0014	14.6±1.3	0.0263±0.0014

$$\frac{z_0^{(i)}}{z_0^{(j)}} = \frac{(1 + R_i)(1 - R_j)}{(1 - R_i)(1 + R_j)}, \quad \frac{T^{(i)}/J_+^{(i)}(L^-)}{T^{(j)}/J_+^{(j)}(L^-)} = \frac{1 - R_i}{1 - R_j} \quad (11)$$

Here indices i, j correspond to the reflection coefficient $R_{i,j}$. The comparison of data for any pair of reflectors allows us to find their reflectivities using Eqs. (11). We then use the values of z_0 from Table II and Eq. (4) to find the mean free path. Since there are three combinations of pairs of reflectors we have three separate determinations of the mean free path. These results are presented in Table III. Taking the average value of l from Table III gives $l = 6.43 \pm 0.27$ cm.

The transport velocity is found from a determination of the diffusion coefficient obtained by fitting the photon diffusion model to measurements of the intensity autocorrelation and cross-correlation functions with frequency shift in the 18–19 GHz range using the value of α from Table II and D as a fitting parameter. The theoretical expressions for the correlation functions include the field factorization term and the leading-order correction found by the Langevin approach.^{16,17} The fit gives $D = (4.0 \pm 0.2) \times 10^{10}$ cm²/s and $v = 3D/l = (1.86 \pm 0.18) \times 10^{10}$ cm/s. This value of v is 25% less than the effective-medium approximation, indicating that microscopic resonances in the sample significantly retard energy transport even in the present high-density limit.

The adequacy of the photon diffusion theory near the output surface is tested by relating intensity values at the sample surface to the transmission for the three reflectors. From the boundary conditions (2) and Eq. (10) we get a relationship between the total transmission and the intensity at the output boundary,

$$T(L)z_0/I(L^-) = D/q \quad (12)$$

This ratio is independent of the surface reflectivity. $I(L^-)$ is obtained from the extrapolation of the lines in Fig. 2 to $L - z = 0$. The consistency of our experiments with the predictions of diffusion theory can be verified by taking $T(L)$, $I(L^-)$, and z_0 and checking to see if the ratio in Eq. (12) gives a constant result for the three reflectors. In our experiments we measure relative values of total transmission $\tilde{T}(L)$ and intensity $\tilde{I}(z)$ and moreover q is not known. Thus the ratio of Eq. (12) does not give the diffusion constant but only a constant \tilde{D} proportional to D . The value of \tilde{D} , however, should not depend on reflectivity. The values of $\tilde{T}(L)$, $\tilde{I}(L^-)$, z_0 , and \tilde{D} are listed in Table I. To within 3%, \tilde{D} does not depend on

TABLE III. Values of the mean free path and reflection coefficients recovered from Eqs. (11) and (4). In the first column pairs of reflection coefficients used in Eq. (11) to obtain each value of l are indicated.

	R_1	R_2	R_3	l (cm)
R_1, R_2	0.155	0.364	0.524	6.11
R_1, R_3	0.132	0.343	0.507	6.40
R_2, R_3	0.104	0.318	0.486	6.77

internal reflectivity as predicted by diffusion theory. Similar results were obtained using different "integrating boxes."

In conclusion, we find that the extrapolation of intensity measurements in the interior of a sample to the output surface are in excellent agreement with measurements of transmission through the sample when these results are described by photon diffusion theory with appropriate boundary conditions. These results show that diffusion theory gives a *quantitative* description of electromagnetic propagation from the bulk to the output surface. This al-

lows us to determine the transport mean free path and the internal reflectivity. A comparison with measurements of the diffusion coefficient allows us to determine the transport velocity, which gives the connection between dynamic and static transport parameters.

This work is supported by the NSF under Grant No. DMR-9001335, by the Petroleum Research Fund of the ACS under Grant No. 22800-AC,7 and by the PSC-CUNY under Award No. 662372.

-
- ¹S. Glasstone and M. C. Edlund, *The Elements of Nuclear Reactor Theory* (Van Nostrand, New York, 1952).
- ²P. M. Morse and H. Feshbach, *Methods of Theoretical Physics* (McGraw-Hill, New York, 1953).
- ³E. Akkermans, P. E. Wolf, and R. Maynard, Phys. Rev. Lett. **56**, 1471 (1986).
- ⁴F. C. MacKintosh and S. John, Phys. Rev. B **40**, 2283 (1989).
- ⁵M. P. Van Albada and A. Lagendijk, Phys. Rev. Lett. **55**, 2692 (1985).
- ⁶P. E. Wolf and G. Maret, Phys. Rev. Lett. **55**, 2696 (1985).
- ⁷M. Kaveh, M. Rosenbluh, I. Edrei, and I. Freund, Phys. Rev. Lett. **57**, 2049 (1986).
- ⁸S. Feng, C. Kane, P. A. Lee, and A. D. Stone, Phys. Rev. Lett. **61**, 834 (1988).
- ⁹I. Freund, M. Rosenbluh, and S. Feng, Phys. Rev. Lett. **61**, 2328 (1988).
- ¹⁰A. Z. Genack, Phys. Rev. Lett. **58**, 2043 (1987).
- ¹¹R. Vreeker, M. P. Van Albada, R. Sprik, and A. Lagendijk, Phys. Lett. A **132**, 51 (1988).
- ¹²J. M. Drake and A. Z. Genack, Phys. Rev. Lett. **63**, 259 (1989).
- ¹³B. Shapiro, Phys. Rev. Lett. **57**, 2168 (1986).
- ¹⁴M. J. Stephen and G. Cwilich, Phys. Rev. Lett. **59**, 285 (1987).
- ¹⁵A. Z. Genack, N. Garcia, and W. Polkosnik, Phys. Rev. Lett. **65**, 2129 (1990).
- ¹⁶R. Pnini and B. Shapiro, Phys. Lett. A **157**, 265 (1991).
- ¹⁷E. Kogan and M. Kaveh, Phys. Rev. B **45**, 1049 (1992).
- ¹⁸M. P. van Albada, J. F. de Boer, and A. Lagendijk, Phys. Rev. Lett. **64**, 2787 (1990).
- ¹⁹G. Maret and P. E. Wolf, Z. Phys. B **65**, 409 (1987).
- ²⁰D. J. Pine, D. A. Weitz, G. Maret, P. E. Wolf, E. Herbolzhmeimer, and P. M. Chaikin, in *The Scattering and Localization of Classical Waves*, edited by P. Sheng (World Scientific, Singapore, 1990).
- ²¹A. Lagendijk, R. Vreeker, and P. de Vries, Phys. Lett. A **136**, 81 (1989).
- ²²I. Freund and R. Berkovits, Phys. Rev. B **41**, 496 (1990); **41**, 9540(E) (1990).
- ²³N. Garcia, J. H. Li, W. Polkosnik, T. D. Cheung, P. Tsang, A. A. Lisyansky, and A. Z. Genack, Physica B **175**, 9 (1991).
- ²⁴J. X. Zhu, D. J. Pine, and D. A. Weitz, Phys. Rev. A **44**, 3948 (1991).
- ²⁵P. M. Saulnier and G. H. Watson (unpublished).
- ²⁶M. P. van Albada, B. A. Tiggelen, A. Lagendijk, and A. Tip, Phys. Rev. Lett. **66**, 3132 (1991).

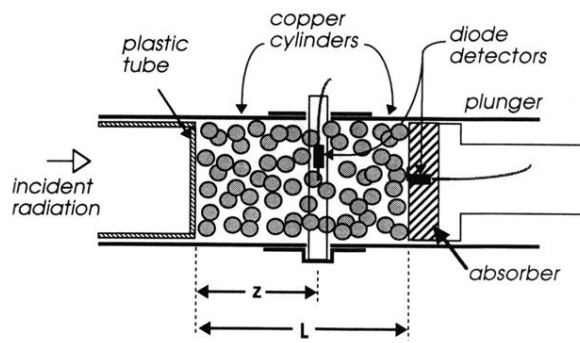


FIG. 1. Schematic of experimental setup used to measure the intensity profile inside the sample.

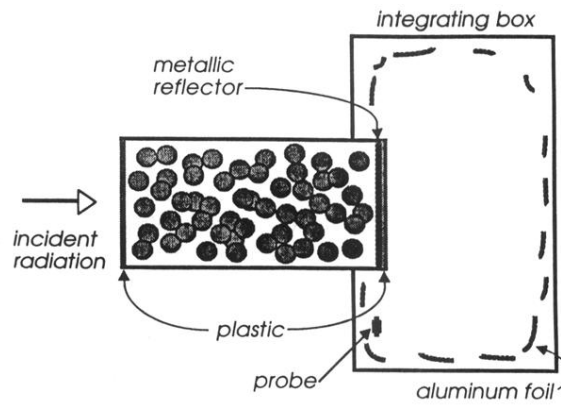


FIG. 3. Schematic of the experimental setup used to measure the relative transmission through the sample.